Journal of Dental Sciences 20 (2025) 2265–2272

Available online at www.sciencedirect.com

ScienceDirect

journal homepage: www.e-jds.com

Original Article

MicroRNA let-7a mitigates the progression of oral submucous fibrosis by targeting high-mobility group AT-hook 2

Hui-Wen Yang [a,b†], Chih-Yuan Fang [c,d†], Shih-Chi Chao [e,f], Yi-Wen Liao [e,f], Cheng-Chia Yu [a,b,f**], Yu-Wei Chiu [a,b*]

[a] School of Dentistry, Chung Shan Medical University, Taichung, Taiwan
[b] Department of Dentistry, Chung Shan Medical University Hospital, Taichung, Taiwan
[c] School of Dentistry, College of Oral Medicine, Taipei Medical University, Taipei, Taiwan
[d] Department of Oral and Maxillofacial Surgery, Wan Fang Hospital, Taipei Medical University, Taipei, Taiwan
[e] Department of Medical Research, Chung Shan Medical University Hospital, Taichung, Taiwan
[f] Institute of Oral Sciences, Chung Shan Medical University, Taichung, Taiwan

Received 28 April 2025; Final revision received 24 May 2025
Available online 12 June 2025

KEYWORDS
Oral submucous fibrosis;
Myofibroblasts;
Arecoline;
microRNA;
Let-7a;
HMGA2

Abstract *Background/purpose:* Oral submucous fibrosis (OSF) is an irreversible fibrotic disorder of the oral cavity with a high potential for malignant transformation. MicroRNA lethal-7a (let-7a) has been recognized as a key antifibrotic regulator, but its specific role in OSF remains unknown. Therefore, this study aimed to elucidate the functional significance and the molecular mechanism of let-7a in OSF progression.
Materials and methods: The expression of let-7a was quantified by real-time quantitative polymerase chain reaction in fibrotic buccal mucosal fibroblasts (fBMFs) isolated from OSF lesions and patient–matched non-fibrotic BMFs (BMFs). Myofibroblastic characteristics were evaluated using collagen-gel contraction, Transwell migration, and wound-healing assays. Restoration and inhibition of let-7a expression were achieved by transfecting let-7a mimics or inhibitors, respectively. Direct binding of let-7a to high-mobility group AT-hook 2 (HMGA2) mRNA was verified using luciferase reporter assay.
Results: Let-7a expression was significantly down-regulated in fBMFs isolated from OSF lesions compared with patient–matched non-fibrotic BMFs. Moreover, let-7a expression declined in a dose–dependent manner during arecoline–induced myofibroblastic transdifferentiation of

* Corresponding author. School of Dentistry, Chung Shan Medical University, No. 110, Sec. 1, Jianguo N. Rd., Taichung 40201, Taiwan.
** Corresponding author. Institute of Oral Sciences, Chung Shan Medical University, No. 110, Sec. 1, Jianguo N. Rd., Taichung 40201, Taiwan.
E-mail addresses: ccyu@csmu.edu.tw (C.-C. Yu), dentalhandsomeboy@gmail.com (Y.-W. Chiu).
† These two authors contributed equally to the results of this study.

https://doi.org/10.1016/j.jds.2025.05.027

BMFs. Myofibroblastic characteristics, including cell contractility, cell migration, and wound-healing capacity were significantly decreased in fBMFs after transfection of let-7a mimics. Mechanistically, let-7a directly targeted the HMGA2 mRNA, leading to post-transcriptional repression of HMGA2. Importantly, silencing of HMGA2 was sufficient to diminish cell contractility and myofibroblasts marker expression in fBMFs.
Conclusion: The present study demonstrates that let-7a suppresses oral myofibroblast activation by directly targeting HMGA2. This finding first establishes the let-7a/HMGA2 axis as a promising therapeutic target for mitigating the progression of OSF.

Introduction

Oral submucous fibrosis (OSF) is a chronic and progressive fibrotic disorder of the oral mucosa characterized by persistent inflammation, excessive collagen deposition, and consequent mucosal stiffening that ultimately restricts mouth opening.[1,2] Oral submucous fibrosis disproportionately affects East and Southeast Asian populations, where betel-quid chewing is culturally entrenched.[1,2] In Taiwan, a 17-year epidemiological survey showed the prevalence of OSF rising from 8.3 % to 16.2 %.[3] Moreover, a meta-analysis has estimated that 4.2 % of OSF cases undergo malignant transformation to oral cancer,[4] indicating OSF as an oral potentially malignant disorder (OPMD). These data emphasize the ongoing clinical challenge despite medical advances.

Arecoline, the major alkaloid in areca nuts, can drive the myofibroblastic transdifferentiation of oral fibroblasts by activating various pro-fibrogenic mechanism such as the transforming growth factor (TGF)-β1/Smad2 signaling pathway. Myofibroblasts are recognized as key contributors in fibrotic diseases through overproduction of extracellular matrix (ECM) components and elevated ECM contractility, thereby promoting the formation of fibrotic bundles and perpetuating OSF progression. Indeed, α-smooth muscle actin (α-SMA), a key myofibroblast marker, has been found to be predominantly expressed in the lamina propria of fibrotic mucosa in OSF patients, rather than in areas of fibroepithelial hyperplasia,[5] and it has been confirmed that the expression intensity of α-SMA significantly increased with disease progression.[6,7] Hence, targeting myofibroblast activation is considered a promising strategy for mitigating OSF.

MicroRNAs (miRNAs) are small non-coding RNAs (ncRNAs) of approximately 22 nucleotides that suppress gene expression at post-transcriptional level by binding to complementary seed-sequence within the 3 prime untranslated region (3′-UTR) of their specific targets.[8] The lethal-7 (let-7) family, first described in *Caenorhabditis elegans*, participates in diverse biological processes, including immune modulation,[9] carcinogenesis,[10] neurodegeneration,[11] and fibrogenesis.[12–15] Previous studies of diabetic nephropathy have shown that advanced glycation end-products markedly suppressed let-7a in mesangial cells, which in turn activated a myeloid differentiation primary response (MyD)-88–dependent inflammatory cascade and pro-fibrogenic phenotype changes.[14] Likewise, a study of ischemia–induced atrial fibrosis demonstrated that let-7a was reduced in cardiomyocytes under hypoxic condition, thereby relieving the repression of type I collagen A1 (COL1A1) and COL3A1 and promoting collagen excessive production.[15] Notably, let-7a has also been reported to govern the physiological and pathological processes in oral tissues. For instance, let-7a fostered the osteogenic differentiation of bone-marrow mesenchymal stem cells (BMSCs) to support the periodontal bone regeneration,[16] whereas its down-regulation increased tumour–initiating capacity in oral squamous cell carcinoma (OSCC) cells.[17] Despite these observations, the specific role of let-7a in regulating the OSF progression remains unclear.

The present study confirmed the significantly diminished expression of let-7a in primary fBMFs, as well as in arecoline-induced myofibroblastic differentiation of non-fibrotic BMFs. We further elucidated that let-7a exerted its inhibitory effects on myofibroblast characteristics by directly targeting the high mobility group AT-hook 2 (HMGA2). Our findings delineated a critical let-7a/HMGA2 regulatory axis in the pathogenesis of oral fibrogenesis. Through this work, we provided preclinical evidence supporting the potential of targeting the let-7a/HMGA2 axis as a novel approach against OSF.

Materials and methods

Tissue specimen collection and primary culture

The study adhered to the principles of the Declaration of Helsinki and was approved by the Institutional Review Board of Chung Shan Medical University Hospital. Written informed consent was obtained from all participants before biopsy. Paired specimens of non-fibrotic buccal mucosa and fibrotic bands were collected from five clinically and histologically confirmed OSF patients. Each specimen was transferred on ice in Dulbecco's Modified Eagle Medium (DMEM) supplemented with 1 % penicillin–streptomycin cocktail and either processed immediately or stored at −80 °C until use. Buccal samples were minced into fragments (<1 mm^3) and digested with 0.05 % trypsin–EDTA for 30 min at 37 °C. After centrifugation, the tissue pellet was

plated into T-25 culture flasks and cultured for 10 days in DMEM containing 10 % fetal bovine serum (FBS), 1 % penicillin–streptomycin cocktail, and 2 mM L-glutamine. Spindle–shaped cells migrating from the explants were regarded as fibroblasts and subcultured once 70–80 % confluence had been reached. Fibroblasts obtained from non-fibrotic tissue were identified as buccal mucosal fibroblasts (BMFs). Fibrotic BMFs (fBMFs) were obtained from fibrotic bands and subsequently confirmed to exhibit higher expression of myofibroblast markers (α-SMA and COL1A1), as well as to display enhanced collagen-gel contractility. Primary cultures at passages 3–8 was used for all subsequent experiments. A 10 mg/mL stock solution of arecoline hydrobromide (Sigma–Aldrich, St. Louis, MO, USA) was freshly prepared in phosphate buffered saline (PBS), sterile–filtered through a 0.22 μm membrane, and stored at −20 °C. To induce myofibroblastic transdifferentiation, BMFs were exposed in DMEM containing arecoline at final concentrations of 0, 5, 10, or 20 μg/mL for 48 h. Unless otherwise stated, all reagents were obtained from Gibco (Thermo Fisher Scientific, Waltham, MA, USA).

Real-time quantitative polymerase chain reaction

Total RNA, including the small RNA fraction, was isolated with the mirVana™ PARIS kit (Invitrogen, Thermo Fisher Scientific) in accordance with the manufacturer's instructions. For miRNA analysis, 10 ng of RNA was reverse-transcribed using the TaqMan™ MicroRNA Reverse Transcription Kit (Applied Biosystems, Thermo Fisher Scientific) together with the assay–specific stem-loop primer. For mRNA analysis, 1 μg of RNA was reverse-transcribed with the SuperScript™ III First-Strand Synthesis System (Invitrogen) and random hexamers. Real-time quantitative polymerase chain reaction (RT–qPCR) was performed on a 7900HT Fast Real-Time PCR System (Applied Biosystems) using TaqMan™ MicroRNA Assays (Applied Biosystems) for miRNA reactions and PowerUp™ SYBR Green Master Mix (Applied Biosystems) for mRNA reactions. The specific primers are listed: HMGA2 forward 5′-TCCCTCTAAAGCAGCTCAAAA-3′, reverse 5′-ACTTGTTGTGGCCATTTCCT-3'; GAPDH forward 5′-CTCATGACCACAGTCCATGC-3′, reverse 5′-TTCAGCTCTGGGATGACCTT-3'. Relative gene expression levels were calculated using the $2^{-\Delta Ct}$ method.

Let-7a overexpression and inhibition

Cells were transfected with let-7a mimics, let-7a inhibitor, or equal concentrations of scrambled non-targeting controls (miR-Scr., Applied Biosystems) using Lipofectamine 2000 (Invitrogen). Transfection efficiency was confirmed with Cy3–labeled control oligos (Applied Biosystems).

Western blotting analysis

Whole cell lysates were prepared in RIPA buffer (Millipore, Merck, Darmstadt, Germany) with protease/phosphatase inhibitors cocktail (Roche, Basel, Switzerland). Protein concentration was determined using Bradford assay (Bio-Rad Laboratories, Hercules, CA, USA). Twenty μg of protein per lane was separated on 10 % SDS-PAGE, electrotransferred to PVDF membranes (0.45 μm; Millipore), and blocked with 5 % bovine serum albumin (Sigma–Aldrich) for 1 h at room temperature. Membranes were incubated overnight at 4 °C with primary antibodies including anti-α-SMA (Novus Biologicals, Centennial, CO, USA), anti-HMGA2 (Abcam, Cambridge, UK), anti-GAPDH (Invitrogen). After washing, HRP-conjugated secondary antibodies (Millipore) were applied for 1 h at room temperature. Chemiluminescent bands were developed using an enhanced chemiluminescence substrate (T-Pro Biotechnology, Taipei, Taiwan) and visualized using the LAS-4000 mini analyzer (GE Healthcare, Chicago, IL, USA). Densitometric analysis was performed in ImageJ software (National Institutes of Health, Bethesda, MD, USA).

Collagen-gel contraction assay

A 500 μL collagen-cell mixture containing 750 μg neutralized type I collagen (Sigma–Aldrich) with 2.5×10^5 cells was added in 24-well plates and allowed to polymerize for 30 min at 37 °C/5 % CO_2. The gels were gently detached and incubated in medium for an additional 48 h. Gel areas were photographed under an inverted microscope and quantified with ImageJ (National Institutes of Health). Gel contraction (%) was calculated as [(initial area − final area)/initial area] × 100.

Wound-healing assay

Confluent monolayers cultured in 6-well plates were linear-scratched with a 200 μL pipette tip. Detached cells were removed by rinsing twice with PBS, and cell images were captured at 0 and 48 h under an inverted microscope.

Luciferase reporter assays

The wild-type (wt) HMGA2 3′-UTR and a mutant (mut) version carrying an 8-nt substitution in the let-7a seed region were PCR-amplified and cloned downstream of firefly luciferase in pmirGLO (Promega, Madison, WI, USA). Cells were co-transfected with luciferase reporter and let-7a mimics or miR-Scr using Lipofectamine 2000 (Invitrogen). After 48 h of incubation at 37 °C/5 % CO_2, firefly and *Renilla* luciferase activities were measured using on an Infinite 200 PRO reader (Tecan, Männedorf, Switzerland).

Transwell migration

A total of 1×10^5 cells suspended in 200 μL serum-free medium was added into 8-μm Transwell inserts (Corning, Corning, NY, USA). The lower chambers were filled with 600 μL medium containing 10 % FBS, which served as the chemoattractant. After 48 h of incubation at 37 °C/5 % CO_2, non-migrated cells on the upper surface of each insert were removed with cotton swabs. The migrated cells on the underside were fixed with 4 % paraformaldehyde e and stained with 0.1 % crystal violet. Crystal-violet bound to migrated cells was eluted in 10 % acetic acid, and absorbance was measured at 590 nm using an Infinite 200 PRO reader (Tecan). Relative migration ability of each test was

expressed as a percentage of the group of fBMFs transfected with miR-Scr.

Lentivirus-mediated knockdown of HMGA2

The pLV-RNAi lentiviral vector encoding short-hairpin targeting HMGA2 (Sh-HMGA2) or a non-targeting luciferase control (Sh-Luc) were obtained from BioSettia (San Diego, CA, USA). Lentiviral particles were produced in 293T cells by co-transfecting the pLV-RNAi construct with packaging and envelope plasmids. Viral supernatants were harvested and concentrated by ultracentrifugation. Fibrotic BMFs were infected with in polybrene and selected with puromycin for 5 days. Knockdown efficiency was verified by RT—qPCR. The specific sequences of Sh-HMGA2 listed as follows: Sh-HMGA2-1: 5′-AAAAGCAGGAACTCAGAAAACTTTTGGATCCAAAAGTTTTCTGAGTTCCTGC-3’; Sh-HMGA2-2: 5′-AAAAGGGACACAATTCACTCCAATTGGATCCAATTGGAGTGAATTGTGTCCC-3’.

Statistical analysis

Results are expressed as mean ± standard deviation (SD). Differences between two groups were analyzed with paired or two-sample two-tailed Student *t*-tests. For comparisons involving more than two groups, a one-way ANOVA followed by Tukey honest significant difference post-hoc testing was applied. Values of $P < 0.05$ were considered statistically significant. All analyses were performed with GraphPad Prism 10 (GraphPad Software, Boston, MA, USA).

Results

To determine whether let-7a functions as an anti-fibrotic miRNA in OSF, we first compared its expression levels in primary buccal mucosal fibroblasts derived from non-fibrotic tissue (BMFs) with the patient-paired fibrotic BMFs (fBMFs). Real time qPCR revealed a significant decrease in let-7a across all five patient pairs (Fig. 1A). We next ask whether the myofibroblastic transdifferentiation of BMFs requires let-7a downregulation. Primary BMFs from two OSF patients were exposed to 0—20 μg/mL arecoline for 48 h (Fig. 1B). Let-7a levels declined in a dose-dependent manner, with significant reductions at 10 and 20 μg/mL (Fig. 1B).

To investigate whether restoring let-7a reverses the myofibroblastic characteristics, the synthetic let-7a mimics were transfected into two independent fBMFs (Fig. 2A). As measured by cellular function assays, the collagen-gel contractility (Fig. B), cell motility (Fig. C), and wound-healing ability (Fig. D) of fBMFs were significantly reduced by let-7a mimics.

To determine the specific anti-fibrotic role of let-7a in fBMFs and BMFs during the myofibroblast trans-differentiation, we searched for direct targets of let-7a. Bioinformatic analysis identified a conserved let-7a seed site within the 3′-UTR of HMGA2 mRNA (Fig. 3A) and the direct binding between let-7a and HMGA2 3′-UTR in fBMFs was verified using luciferase reporter assays (Fig. 3B). Overexpressing let-7a by let-7a mimics transfection was sufficient to suppress luciferase activity from the wild-type HMGA2 3′-UTR reporters (wt-HMGA2) in fBMFs, whereas mutation of the let-7a seed site (mut-HMGA2) abolished this response (Fig. 3B). Consistently, overexpression of let-7a reduced endogenous HMGA2 protein expression in fBMFs, while inhibition of let-7a in BMFs by let-7a inhibitors transfection resulted in an opposite effect on HMGA2 expression (Fig. 3C and D). To examine whether the anti-fibrotic effect of let-7a was achieved by targeting HMGA2, we silenced HMGA2 in fBMFs by lentiviral—mediated expressing Sh-HMGA2. Western blotting analyses showed that silencing HMGA2 markedly decreased the expression of α-SMA (a hallmark of myofibroblasts, Fig. 4A) and significantly diminished the collagen-gel contractility in fBMFs (Fig. 4B). Taken together, these findings demonstrate that HMGA2 is a direct downstream effector of let-7a, and that dysregulation of this axis is essential for maintaining the myofibroblastic characteristics in OSF—derived fBMFs.

Discussion

In this study, we found that let-7a were significantly downregulated in OSF patient—derived fBMFs that exhibit myofibroblastic characteristics. Further investigation showed that arecoline stimulation decreased let-7a expression in primary BMFs in a dose-dependent manner.

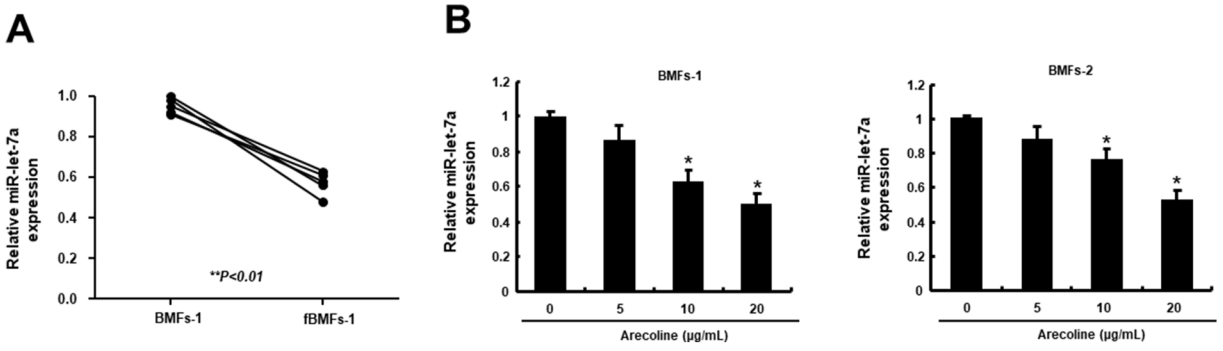

Figure 1 Arecoline-stimulation decreased let-7a expression in primary buccal mucosal fibroblasts.
(A) Relative miR-let-7a expression in primary non-fibrotic buccal mucosal fibroblasts (BMFs) and paired fibrotic BMFs (fBMFs) from five OSF patients was quantified by RT—qPCR. (B) Primary BMFs from two patients (−1; −2) were treated with arecoline (0—20 μg/mL) for 48 h and analysed as in (A). Data are mean ± SD (n = 3). *$P < 0.05$ vs 0 μg/mL arecoline.

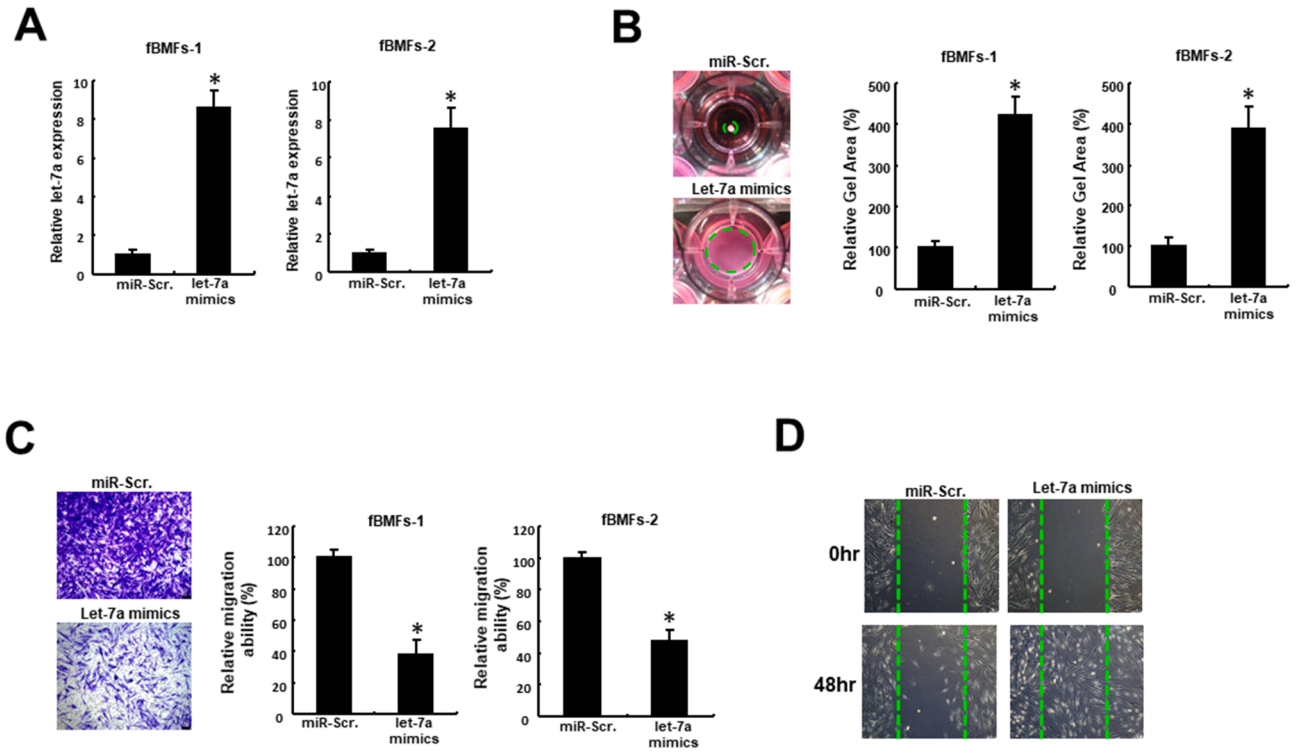

Figure 2 Ectopic let-7a impaired the myofibroblastic characteristics of primary fibrotic buccal mucosal fibroblasts.
(A) Relative let-7a expression in fBMFs (−1; −2) after transfection with let-7a mimics or scrambled control (miR-Scr.) was quantified by RT–qPCR. (B–C) Relative ECM contractility (B), cell motility (C), and wound-healing ability (D) in fBMFs after transfection with let-7a mimics or miR-Scr were assessed using collagen-gel contraction assay (B), Transwell migration system (C), and scratch-wound closure methods (D), respectively. Data are mean ± SD (n = 3). *$P < 0.05$ vs miR-Scr.

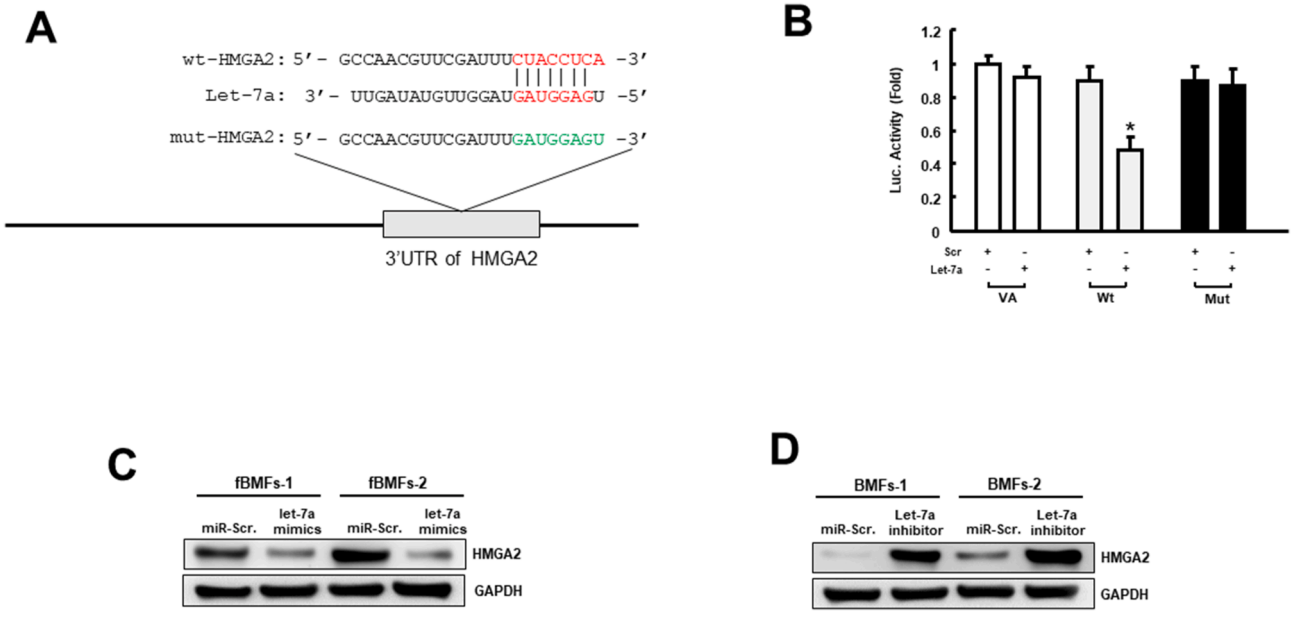

Figure 3 Let-7a directly targeted HMGA2 mRNA.
(A) Schematic showing the predicted let-7a binding site in the HMGA2 3′-UTR (wt-HMGA2) and the corresponding mutant sequence (mut-HMGA2). (B) Luciferase reporter genes activity in fBMFs after co-transfection with vector alone (VA), wild-type (wt) or mutant (mut) HMGA2 3′-UTR reporters plus let-7a mimics or scramble (miR-Scr). Data are mean ± SD (n = 3). *$P < 0.05$ vs miR-Scr. (C) Protein abundance of HMGA2 in fBMFs (−1; −2) after transfection with let-7a mimics or miR-Scr. (D) Protein abundance of HMGA2 in BMFs (−1; −2) after transfection with let-7a inhibitor or miR-Scr.

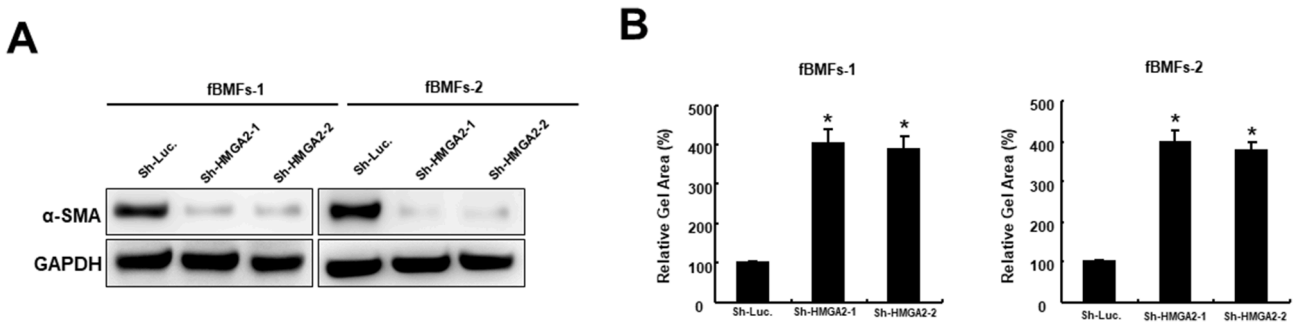

Figure 4 Silencing HMGA2 attenuated myofibroblastic characteristics of primary fibrotic buccal mucosal fibroblasts. (A–B) Protein abundance of α-SMA (A) and relative ECM contractility (B) in fBMFs (−1; −2) expressing Sh-HMGA2 or non-target control (Sh-Luc.) were assessed using Western blotting (A) and collagen-gel contraction assay (B), respectively. Data are mean ± SD (n = 3). *$P < 0.05$ vs Sh-Luc.

Notably, overexpressing let-7a markedly impaired key myofibroblast features in fBMFs, including ECM contractility, cell motility, and wound healing capacity. We further identified HMGA2 mRNA as a direct target of let-7a and revealed a pivotal let-7a/HMGA2 axis that controls myofibroblastic characteristics in OSF progression.

Previous study reported that let-7a was significantly reduced in both the serum and serum-derived extracellular vesicles (EVs) from patients with chronic hepatitis C, with the degree of downregulation correlating with hepatic fibrosis severity.[18] These finding suggest that let-7a could serve as a diagnostic and prognostic biomarker for fibrotic diseases. Notably, a recent study likewise revealed markedly lower salivary let-7a levels in patients with head and neck cancer than in healthy individuals.[19] Therefore, we propose that let-7a holds great potential as a non-invasive biomarker for oral diseases, particularly in the context of areca nut–related fibrotic pathology and malignant transformation.

HMGA2 is a chromatin–associated transcriptional regulator implicated in several pathophysiological processes, such as aging,[20] cancer progression,[21] and diverse fibrotic disorders.[22–24] For instance, HMGA2 was overexpressed in renal tissues from patients with diabetic nephropathy, and silencing HMGA2 reversed the myofibroblastic phenotype and reduced pro-inflammatory factor secretion in glomerular mesangial cells under high glucose conditions.[22,23] Similarly, inhibiting HMGA2 by delivering miR-490-3p mimics reduced TGF-β–induced myofibroblastic features in renal epithelial cells in vitro and significantly alleviated unilateral ureteral obstruction–induced renal injury and fibrosis in vivo.[24] Consistent with these findings, our study demonstrated that silencing HMGA2 markedly suppressed α-SMA expression and collagen-gel contractility in fBMFs (Fig. 4), confirming HMGA2 as a critical pro-fibrogenic factor in regulating myofibroblastic characteristics during OSF progression.

HMGA2 has also been recognized as a key regulator of epithelial-to-mesenchymal transition (EMT).[25] The EMT transcription factor Snail family transcriptional repressor 2 (SNAI2) is among its direct targets, and silencing HMGA2 effectively reduced SNAI2 expression. This, in turn, prevented palmitic acid–induced inflammatory responses and lipid accumulation in hepatocytes, as well as blocked TGF-β1–driven hepatic stellate cell activation.[26] Myofibroblasts can originate not only from direct transdifferentiation of fibroblasts but also through EMT process in multiple cell types.[27] For instance, inhibiting N6-methyladenosine modification of HMGA2 mRNA reduced its stability, thereby preventing TGF-β2–induced EMT and the myofibroblastic transformation of retinal pigment epithelial cells.[28] Furthermore, HMGA2 overexpression was detected in the endometrial tissue of patients with intrauterine adhesions (IUA).[29] Silencing HMGA2 not only reversed TGF-β1–induced EMT and the expression of myofibroblastic markers in endometrial epithelial cells, but also attenuated endometrial fibrosis in IUA mice.[29] Additionally, the long non-coding RNA (lncRNA) H19 can function as a competing endogenous RNA (ceRNA) that sequestered let-7a from HMGA2 mRNA (H19/let-7a/HMGA2 axis) and thereby driven the EMT and the metastatic properties in tongue squamous cell carcinoma cells.[30] Of note, our previous work demonstrated that arecoline stimulation induced the myofibroblastic transdifferentiation of primary BMFs and is accompanied by H19 upregulation. This finding may explain the dose-dependent decrease in let-7a in BMFs upon arecoline stimulation (Fig. 1), probably attributable to elevated H19 acting as a ceRNA that inhibited let-7a. Another study also found that arsenic exposure promoted M2 macrophage polarization and increased TGF-β secretion through the H19/let-7a/c-Myc axis, contributing to pulmonary fibrosis.[31] Taken together, these findings imply that targeting let-7a could not only inhibit the myofibroblastic characteristics of fBMFs but also suppress pro-fibrotic phenotypes in other cells involved in OSF, or prevent their transdifferentiation into myofibroblasts, thereby impeding the OSF progression and potentially lowering the risk of malignant transformation.

Let-7a is itself negatively regulated by lin-28 homolog B (LIN28B), yet it also directly targets LIN28B, forming a negative feedback loop.[32] Disrupting this feedback loop suppressed HMGA2 expression and prevented alcohol–induced hepatic stellate cell activation, thus ameliorating alcoholic hepatic fibrosis in mice.[32] Therefore, we propose that the arecoline-induced upregulation of LIN28B in head and neck cancer cells reported in our previous study may result from the interplay between LIN28B and let-7a.[33] Notably, a recent AlphaScreen–based study

showed that epigallocatechin gallate (EGCG) potently inhibited the LIN28B/let-7a interaction.[34] This study further demonstrated that EGCG significantly up-regulated let-7a expression in neuroblastoma cells and effectively reduced their tumorigenic potential in vivo.[34] EGCG also promoted let-7a expression in preadipocytes and suppresses excessive cell proliferation via the let-7a/HMGA2 axis.[35] In fact, EGCG has been confirmed to prevent the arecoline-induced transdifferentiation of BMFs into myofibroblasts.[36,37] Therefore, our future research is warranted to elucidate the precise role of the LIN28B/let-7a/HMGA2 feedback loop in arecoline-related myofibroblast transformation and OSF progression.

As reported, administering engineered let-7a–enriched EVs derived from Wharton's jelly mesenchymal stem cells (WJ-MSCs) significantly suppressed macrophage infiltration and collagen deposition in rat lung tissues, thereby improving pulmonary function in a rat model of acute lung injury (ALI).[38] This study also showed that co-culturing with these engineered EVs could block TGF-β/Smad signaling and suppress the myofibroblastic characteristics in idiopathic pulmonary fibrosis patient-derived lung fibroblasts without affecting cell proliferation,[38] supporting the safety of exogenous let-7a for therapeutic purposes. Indeed, endogenous let-7a has been confirmed to be preferentially packaged into EVs in MSCs.[39–41] Intra-capsular delivery of bone-marrow MSC-EVs relieved suture-induced shoulder capsular fibrosis and restored joint mobility in mice,[39] whereas adipose-derived MSC-EVs exerted a comparable anti-fibrotic effect in bleomycin-induced scleroderma.[40] Mechanistically, MSC-EVs–let-7a directly targets TGF-βR1 in recipient fibroblasts, which attenuated Smad signaling and diminished myofibroblastic features, such as α-SMA expression, collagen production, and collagen-gel contractility.[39,40] In a spinal cord injury rat model, administration of BMSC–derived EVs enriched with let-7a promoted neuronal repair and limited excessive astroglial scarring by regulating let-7a/HMGA2 axis in astrocytes.[41] Collectively, these findings indicate that let-7a mitigates pathological progression across multiple fibrosis and tissue-repair models, highlighting its therapeutic promise for OSF.

Although this study is the first to identify the significant role of the let-7a/HMGA2 axis in regulating myofibroblast activation in OSF, our findings are primarily obtained from in vitro investigations, which limit the full understanding of the pathology progression in vivo. Nevertheless, our current findings provide a foundation for subsequent translational research. Specifically, we have demonstrated that let-7a expression was significantly down-regulated in fBMFs and exhibited a dose-dependent decrease in BMFs exposed to arecoline treatment. Crucially, the exogenous transfection of let-7a mimics markedly attenuated the myofibroblastic characteristics of fBMFs, supporting the functional importance of let-7a in controlling the persistence of myofibroblasts. Therefore, future research will prioritize the validation of the correlation between let-7a and HMGA2 expression and OSF progression in preclinical animal models and larger patient cohorts. Furthermore, it will be imperative to validate the therapeutic potential of targeting the let-7a/HMGA2 axis within these in vivo settings. Such strategies could include restoring let-7a expression or silencing HMGA2, with a particular focus on their efficacy in inhibiting areca nut-induced fibrotic pathology and preventing subsequent malignant transformation. These could bridge the current translational gap and advance these promising findings towards potential clinical applications in OSF management.

Declaration of competing interest

All authors have no conflicts of interest relevant to this article.

Acknowledgments

This study was supported by grants from Chung Shan Medical University Hospital, Taiwan (grant number: CSH-2023-C-021) and Wan Fang Hospital, Taiwan (grant number: 113-wf-f-5).

References

1. Ray JG, Chatterjee R, Chaudhuri K. Oral submucous fibrosis: a global challenge. Rising incidence, risk factors, management, and research priorities. *Periodontol 2000* 2019;80:200–12.
2. Lee CH, Ko YC, Huang HL, et al. The precancer risk of betel quid chewing, tobacco use and alcohol consumption in oral leukoplakia and oral submucous fibrosis in southern Taiwan. *Br J Cancer* 2003;88:366–72.
3. Yang SF, Wang YH, Su NY, et al. Changes in prevalence of precancerous oral submucous fibrosis from 1996 to 2013 in Taiwan: a nationwide population-based retrospective study. *J Formos Med Assoc* 2018;117:147–52.
4. Kujan O, Mello FW, Warnakulasuriya S. Malignant transformation of oral submucous fibrosis: a systematic review and meta-analysis. *Oral Dis* 2021;27:1936–46.
5. Moutasim KA, Jenei V, Sapienza K, et al. Betel-derived alkaloid up-regulates keratinocyte alphavbeta6 integrin expression and promotes oral submucous fibrosis. *J Pathol* 2011;223:366–77.
6. Angadi PV, Kale AD, Hallikerimath S. Evaluation of myofibroblasts in oral submucous fibrosis: correlation with disease severity. *J Oral Pathol Med* 2011;40:208–13.
7. You Y, Huang Y, Wang D, et al. Angiotensin (1-7) inhibits arecoline-induced migration and collagen synthesis in human oral myofibroblasts via inhibiting NLRP3 inflammasome activation. *J Cell Physiol* 2019;234:4668–80.
8. Kim T, Croce CM. MicroRNA: trends in clinical trials of cancer diagnosis and therapy strategies. *Exp Mol Med* 2023;55:1314–21.
9. Ding X, Du Y, Sun B, et al. MicroRNA let-7a mediates post-transcriptional inhibition of Nr4A1 and exacerbates cardiac allograft rejection. *Cell Signal* 2023;109:110783.
10. Bian Z, Xu C, Xie Y, et al. SNORD11B-mediated 2'-O-methylation of primary let-7a in colorectal carcinogenesis. *Oncogene* 2023;42:3035–46.
11. Zhang J, Dongwei Z, Zhang Z, et al. miR-let-7a suppresses alpha-synuclein-induced microglia inflammation through targeting STAT3 in Parkinson's disease. *Biochem Biophys Res Commun* 2019;519:740–6.
12. Song D, Tang X, Du J, Tao K, Li Y. Diazepam inhibits LPS-induced pyroptosis and inflammation and alleviates pulmonary fibrosis in mice by regulating the let-7a-5p/MYD88 axis. *PLoS One* 2024;19:e0305409.
13. El-Shorbagy AA, Shafaa MW, Salah Elbeltagy R, El-Hennamy RE, Nady S. Liposomal IL-22 ameliorates liver fibrosis through miR-

let7a/STAT3 signaling in mice. *Int Immunopharmacol* 2023;124:111015.
14. Luo Q, Xia X, Luo Q, et al. Long noncoding RNA MEG3-205/Let-7a/MyD88 axis promotes renal inflammation and fibrosis in diabetic nephropathy. *Kidney Dis* 2022;8:231—45.
15. Lo CH, Li LC, Yang SF, et al. MicroRNA let-7a, -7e and -133a attenuate hypoxia-induced atrial fibrosis via targeting collagen expression and the JNK pathway in HL1 cardiomyocytes. *Int J Mol Sci* 2022;23:9636.
16. Yang S, Gao J, Chen M, et al. Let-7a promotes periodontal bone regeneration of bone marrow mesenchymal stem cell aggregates via the Fas/FasL-autophagy pathway. *J Cell Mol Med* 2023;27:4056—68.
17. Chien CS, Wang ML, Chu PY, et al. Lin28B/let-7 regulates expression of Oct4 and Sox2 and reprograms oral squamous cell carcinoma cells to a stem-like state. *Cancer Res* 2015;75:2553—65.
18. Matsuura K, Aizawa N, Enomoto H, et al. Circulating let-7 levels in serum correlate with the severity of hepatic fibrosis in chronic hepatitis C. *Open Forum Infect Dis* 2018;5:ofy268.
19. Fadhil RS, Wei MQ, Nikolarakos D, Good D, Nair RG. Salivary microRNA miR-let-7a-5p and miR-3928 could be used as potential diagnostic bio-markers for head and neck squamous cell carcinoma. *PLoS One* 2020;15:e0221779.
20. Hu Q, Zhang N, Sui T, et al. Anti-hsa-miR-59 alleviates premature senescence associated with Hutchinson-Gilford progeria syndrome in mice. *EMBO J* 2023;42:e110937.
21. Yamamoto N, Dobersch S, Loveless I, et al. HMGA2 expression predicts subtype, survival, and treatment outcome in pancreatic ductal adenocarcinoma. *Clin Cancer Res* 2025;31:733—45.
22. Wang X, Liu Y, Rong J, Wang K. LncRNA HCP5 knockdown inhibits high glucose-induced excessive proliferation, fibrosis and inflammation of human glomerular mesangial cells by regulating the miR-93-5p/HMGA2 axis. *BMC Endocr Disord* 2021;21:134.
23. Dong Q, Dong L, Zhu Y, Wang X, Li Z, Zhang L. Circular ribonucleic acid nucleoporin 98 knockdown alleviates high glucose-induced proliferation, fibrosis, inflammation and oxidative stress in human glomerular mesangial cells by regulating the microribonucleic acid-151-3p-high mobility group AT-hook 2 axis. *J Diabetes Investig* 2022;13:1303—15.
24. Wang L, Wang X, Li G, et al. Emodin ameliorates renal injury and fibrosis via regulating the miR-490-3p/HMGA2 axis. *Front Pharmacol* 2023;14:1042093.
25. Ma Q, Ye S, Liu H, Zhao Y, Mao Y, Zhang W. HMGA2 promotes cancer metastasis by regulating epithelial-mesenchymal transition. *Front Oncol* 2024;14:1320887.
26. Sun J, Jin X, Zhang X, Zhang B. HMGA2 knockdown alleviates the progression of nonalcoholic fatty liver disease (NAFLD) by downregulating SNAI2 expression. *Cell Signal* 2023;109:110741.
27. Kuppe C, Ibrahim MM, Kranz J, et al. Decoding myofibroblast origins in human kidney fibrosis. *Nature* 2021;589:281—6.
28. Wang Y, Chen Y, Liang J, et al. METTL3-mediated m6A modification of HMGA2 mRNA promotes subretinal fibrosis and epithelial-mesenchymal transition. *J Mol Cell Biol* 2023;15:mjad005.
29. Song M, Cao C, Zhou Z, et al. HMGA2-induced epithelial-mesenchymal transition is reversed by let-7d in intrauterine adhesions. *Mol Hum Reprod* 2021;27:gaaa074.
30. Kou N, Liu S, Li X, et al. H19 facilitates tongue squamous cell carcinoma migration and invasion via sponging miR-let-7. *Oncol Res* 2019;27:173—82.
31. Xiao T, Zou Z, Xue J, et al. LncRNA H19-mediated M2 polarization of macrophages promotes myofibroblast differentiation in pulmonary fibrosis induced by arsenic exposure. *Environ Pollut* 2021;268:115810.
32. McDaniel K, Huang L, Sato K, et al. The let-7/Lin28 axis regulates activation of hepatic stellate cells in alcoholic liver injury. *J Biol Chem* 2017;292:11336—47.
33. Lin WT, Shieh TM, Yang LC, Wang TY, Chou MY, Yu CC. Elevated Lin28B expression is correlated with lymph node metastasis in oral squamous cell carcinomas. *J Oral Pathol Med* 2015;44:823—30.
34. Cocchi S, Greco V, Sidarovich V, et al. EGCG disrupts the LIN28B/let-7 interaction and reduces neuroblastoma aggressiveness. *Int J Mol Sci* 2024;25:4795.
35. Chen WT, Yang MJ, Tsuei YW, et al. Green tea epigallocatechin gallate inhibits preadipocyte growth via the microRNA-let-7a/HMGA2 signaling pathway. *Mol Nutr Food Res* 2023;67:e2200336.
36. Hsieh YP, Chen HM, Chang JZ, Chiang CP, Deng YT, Kuo MY. Arecoline stimulated early growth response-1 production in human buccal fibroblasts: suppression by epigallocatechin-3-gallate. *Head Neck* 2015;37:493—7.
37. Hsieh YP, Wu KJ, Chen HM, Deng YT. Arecoline activates latent transforming growth factor beta1 via mitochondrial reactive oxygen species in buccal fibroblasts: suppression by epigallocatechin-3-gallate. *J Formos Med Assoc* 2018;117:527—34.
38. Chen SY, Chen YL, Li PC, et al. Engineered extracellular vesicles carrying let-7a-5p for alleviating inflammation in acute lung injury. *J Biomed Sci* 2024;31:30.
39. Luo Z, Sun Y, Qi B, et al. Human bone marrow mesenchymal stem cell-derived extracellular vesicles inhibit shoulder stiffness via let-7a/Tgfbr1 axis. *Bioact Mater* 2022;17:344—59.
40. Wang L, Li T, Ma X, et al. Exosomes from human adipose-derived mesenchymal stem cells attenuate localized scleroderma fibrosis by the let-7a-5p/TGF-betaR1/Smad axis. *J Dermatol Sci* 2023;112:31—8.
41. Wang Y, Han T, Guo R, et al. Micro-RNA let-7a-5p derived from mesenchymal stem cell-derived extracellular vesicles promotes the regrowth of neurons in spinal-cord-injured rats by targeting the HMGA2/SMAD2 axis. *Front Mol Neurosci* 2022;15:850364.